Next-generation optical microscopy

Rahul Roy*

Department of Chemical Engineering, and Molecular Biophysics Unit, Indian Institute of Science, Bangalore 560 012, India

A new breed of microscopy techniques is coming to the forefront of optical imaging. They enhance the attainable 3D resolution of imaging 'in live and "fixed" cells' (with minimal structural perturbation) by greater than tenfold, bringing subcellular structures in sharp focus. Along with multi-colour, long-term imaging, deep tissue and high throughput capabilities, new insights in various fields of biology are being generated. The main set of these next-generation optical microscopy techniques along with select applications is described in this article.

Keywords: Fluorescence, optical resolution, stimulated emission depletion microscopy, super-resolution microscopy.

Introduction

'SEEING is believing' is given significant credence in biology. Hence, microscopy has been the workhorse of many biology laboratories around the world. While several powerful techniques like scanning electron microscopy (SEM), scanning tunnelling microscopy (STM) and atomic force microscopy (AFM) exist, optical microscopy is extremely popular because of its non-invasive nature and compatibility with live samples. With the extensive use of imaging to characterize and validate biological phenomena today, there is a continuing need to develop new innovations in microscopy. Optical microscopy has undergone several revolutionary changes since its inception. At present, we stand at a juncture that can be termed the beginning of a new era in optical microscopy. This next generation of optical microscopy is bound to transform biological imaging generating new insights and paradigms.

This article discusses how new techniques in optical microscopy are enabling multifold improvement in the informational output from biological imaging. Various aspects regarding super-resolution microscopy (SRM) such as super-resolution probes, super-resolution reconstruction algorithms and non-biological applications have been left out for brevity or when additional reviews exist[1–4]. Also, mostly applications in various fields of biology are discussed where the imaging at 10–100 nm resolution provided new or unexpected insights. Most of the concepts discussed here have been implemented successfully using fluorescence due to its high sensitivity and the availability of good probes. However, most of them are applicable to other microscopy techniques where imaging contrast is generated by the signal produced from the molecules.

*e-mail: rahulroy@chemeng.iisc.ernet.in

Brief historical outline

Optical microscopy has undergone three major phases of development. Construction of the first compound microscope is attributed to the Dutch father and son pair of Johannes and Zaccharias Jansen around the late 1500s. Using a pair of lenses, they showed that 5–10-fold magnification could be achieved. Biological microscopy, however, was really pioneered by Antonie van Leeuwenhoek, who used his skills in glass polishing for lens making and developed his single lens microscopes in the late 1600s. With magnifications of up to 275-fold afforded by these microscopes, Leeuwenhoek imaged biological samples like bacteria and spermatozoa, the banded muscular fibre patterns and discovered the cell vacuole. British researcher Robert Hooke further improved the design to include a user-friendly three-lens geometry, which enabled higher contrast. Based on his observations, Hooke described many insects, eye of a fly, and honeycomb ultra-structure of plant cells that also led him to coin the name 'cell' in his historic book *Micrographia* in 1665 (ref. 5).

The next phase of advancements in optical microscopy came from the understanding of the basic principles of light and its interaction with matter. Between 1720 and 1760 (ref. 6), Chester Moore Hall and John Dollond showed how a combination of multiple lenses could be used to correct chromatic aberration, and in 1825, Joseph Jackson Lister[7] further introduced the idea of using aspheric lenses for correcting spherical aberration. However, it was the commercialization of the lens-making process by Carl Zeiss and Otto Schott around the late 1800s that established microscopy as a tool for scientific enquiry. Their efforts were aided by Ernst Abbe's work on lens design and his formulation of the resolution limit of a microscope[8]. Development of Fourier optics and wave theory led to an enhanced understanding of diffraction and interference and propelled further development of aspheric lenses. Innovations like fluorescence-based contrast enhancement, molecule-specific tagging as well as live organism imaging have since then provided unique insights in diverse fields ranging from cellular

physiology to molecular interactions. Furthermore, confocal as well as multi-photon microscopy allowed optical sectioning that was necessary for 3D imaging of biological samples[9]. For another 100 years or so, the improvements in microscopy still worked with the resolution limits set by the optical properties of glass and the wavelength of light used. However, the understanding of many molecular phenomena in biology still needed probing interactions or structures at the nanometre scale, which was beyond the resolution limit of optical microscopy.

Resolution in optical microscopy or the capability to distinguish 'nearby' features has been addressed more recently in the past couple of decades ushering in a new era of innovations[10]. This review will primarily discuss two major approaches in this area of next-generation optical microscopy that allow imaging of samples with greater than ten-fold improvement in the resolution compared to conventional microscopes. Here, the focus is to draw attention to the impact and potential of such techniques to unravel new biology. Several other potential areas for innovation that might experience similar transformation are described as well.

Limits on resolution

Abbe was one of the first to realize that the highest achievable point-to-point resolution of a microscope was not related to the magnification, but was fundamentally limited by the diffraction of light[11]. Because of the wave nature of light, light passing through an aperture (in case of a microscope, the aperture of the objective) is diffracted and smaller the aperture (or the aperture collection angle, α), larger will be the deviation from the normal (Figure 1 *a*). Hence a point source imaged through a lens will produce a blurred spot (each spot described as the point spread function, PSF) whose radius would depend on the wavelength of the light (λ) and sin α (Figure 1 *b*). Abbe formalized this description to define a resolution limit, which is commonly used today for the radius of the blurred spot

$$d_{x,y} = \lambda/2\eta \sin\alpha \quad (1)$$

where η is the refractive index of the medium and $\eta \sin\alpha$ is termed as the numerical aperture (NA) of the lens (Figure 1 *c*). Since the sample being imaged is comprised of several point-like light sources, the final image will be compounded by the interference among an array of these spots and hence features less than about half of the wavelength of light cannot be distinguished. The resolution along the axial direction is poor, and defined as

$$d_z = 2\lambda/(\eta \sin\alpha)^2. \quad (2)$$

Therefore, even while using a very high NA (= 1.4) and 500 nm (green) light, the lateral and axial resolution is limited to 180 and 500 nm respectively. Reducing this limit using smaller wavelengths (e.g. UV) is not usually feasible due to lack of lens material with good optical properties for UV as well as the lethal nature of such illumination for biological samples. Higher refractive index-based imaging is also hampered by the fact that biological materials (mostly comprised of water, $\eta = 1.33$) themselves form a part of the optical path. While near-field approaches like near-field scanning optical microscope (NSOM)[12] that avoid focusing of light by a lens have been employed to enhance resolution, the inherent necessity to probe specimens in contact (or near-contact) mode has limited its widespread use by biologists.

Several approaches in 'far-field' microscopy have worked around the diffraction-limited resolution problem. For example, using two opposing objectives to simultaneously collect light from the sample increases the axial resolution by effectively doubling the apparent NA of the system in the axial direction. In its point-scanning (4Pi) and widefield (I^5M) incarnations, an improvement of up to sevenfold in axial resolution has been demonstrated[13,14]. However, these ideas only increased the collection efficiency of the optical system and hence were still effectively diffraction-limited.

Another elegant approach to improving the resolution has been through manipulation of the image frequency space. Because of limited resolution, features in the sample image that lie in the high-frequency regime cannot be distinguished. However, interfering the sample with a periodic (or known pattern) of illumination allows the convolution of the pattern with sample features and effectively shifting the information from the sample to a lower frequency space. In practice, this is achieved by translating the position and varying the phase of a grid pattern of illumination to acquire a set of images at each condition. Using 9–15 such images and relying on the known characteristics of the illumination pattern, a higher resolution sample image can be computed[15,16]. This structured illumination microscopy (SIM) family of techniques is best suited for fast imaging with large fields of view. However, since the images are still created by mixing two diffraction-limited patterns, it can successfully achieve only up to a twofold increase in the spatial resolution. Though nonlinearity could be employed to enhance the achievable resolution[17], major limitations remain, especially in the form of photobleaching of probes under intense illumination.

Super-resolution microscopy

While accurate position of single molecules could be determined with high nanometre precision when each molecule is spatially well separated or distinguishable[18], achieving imaging resolution beyond the diffraction limit is complicated due to the overlap of many single-molecule PSFs (Figure 2 *a*). The new breed of super-resolution

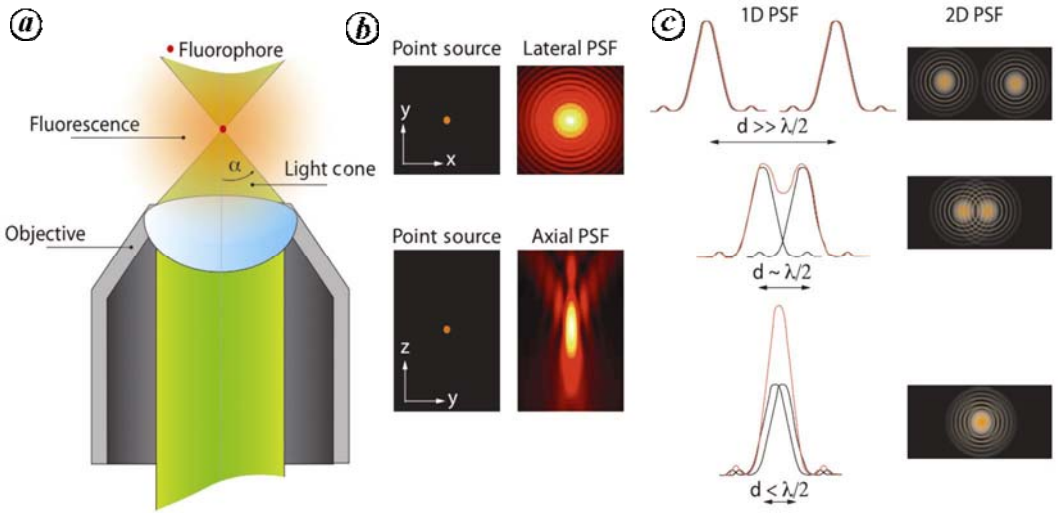

Figure 1. Optical resolution limit. ***a***, Excitation beam (green) can be focused using a lens (or objective) to a narrow region defined by the diffraction limit (eq. (1)). A fluorophore at the focus of the objective when excited by the incoming excitation beam emits fluorescence light isotropically. Larger the light cone angle (or the numerical aperture of the lens), larger is the light collected, but the image of the point-like fluorophore will be blurred due to diffraction to a spot with lateral dimensions of $d_{x,y}$. ***b***, Emission point spread function (PSF) of a point source of light will produce a central peaked function called air disc surrounded by less bright rings laterally (top panel) and a complex elongated pattern axially (bottom panel) when imaged in far-field. ***c***, Optical resolution limit has been largely defined as the minimum distance between two light-emitting molecules that are distinguishable from each other when viewed simultaneously. Since modern optical imaging is done with the numerical aperture close to one, resolution limit is approximately equal to $\lambda/2$. As distance d between two molecules becomes smaller and comparable to $\lambda/2$, they become increasingly difficult to distinguish. Therefore, for optical features smaller than ~ 200 nm, it is hard to resolve them as distance between them is smaller than $\lambda/2$.

techniques takes advantage of the fact that while imaging requires collection of signal from markers from a diffraction-limited spot ($\sim \lambda/2\eta$), this signal can be collected independently from other markers by separating them in time, space, colour or by any other property[10,19]. The breakthrough in imaging beyond the diffraction limit came with the realization that PSF of the imaging system is defined by the convolution of the excitation profile and emission state of the molecules under illumination[20]. By manipulating the emission state of the molecule using a secondary mechanism such that their position is addressable, one can collect light only from a select number of the probes within the diffraction-limited spot. For example, one can sequentially transfer the imaging probes to 'on' or 'bright' state from a previously 'off' or 'invisible' state and collect the signal from the 'on' molecules. The major difference in the two families of super-resolution techniques arises from the way the sub-diffraction positions of the bright molecules are addressed[19,21]. In one family of techniques (reversible saturable optical fluorescence transitions, RESOLFT), the position of the select 'on' molecule(s) is predetermined and usually set to a narrow region in the centre of the excitation beam focus (Figure 2 *b*). Since signal is emitted from a sub-diffractive region of interest, it represents the spatial features of this region and scanning this selective illumination scheme over the sample can generate a super-resolution image (Figure 2 *d*). In another set of techniques, broadly known as stochastic localization and reconstruction microscopy (SLRM), one relies on the capability to determine accurately the position of single molecules post-acquisition and hence requires no control over their temporal sequence of appearance (Figure 2 *c*). The final image is then reconstructed from the individual localization coordinates to approximate the distribution of probes in the sample (Figure 2 *e*). Several strategies to control the 'on'–'off' transition of the markers have resulted in a plethora of techniques in each category[19] and only the major forms of each are discussed in further detail.

RESOLFT microscopy

To control the fraction and location of the marker molecules that contribute to the signal for image creation in a deterministic fashion non-invasively, one must rely on an optical field to act in coordination with the excitation. The best way to define the position of 'bright' molecules is by creating the 'on–off' transition in the vicinity of the illumination PSF. This idea was demonstrated by Stefan Hell's group in stimulated emission depletion (STED) microscopy and has spawned a family of similar techniques known broadly as RESOLFT microscopy[20,22,23]. In its simplest form, STED relies on inducing a dark state such that all the probes, except those in the centre of the illumination PSF are sent to the dark state[24]. This is achieved using illumination from a separate STED laser to induce transition of the excited molecules to the

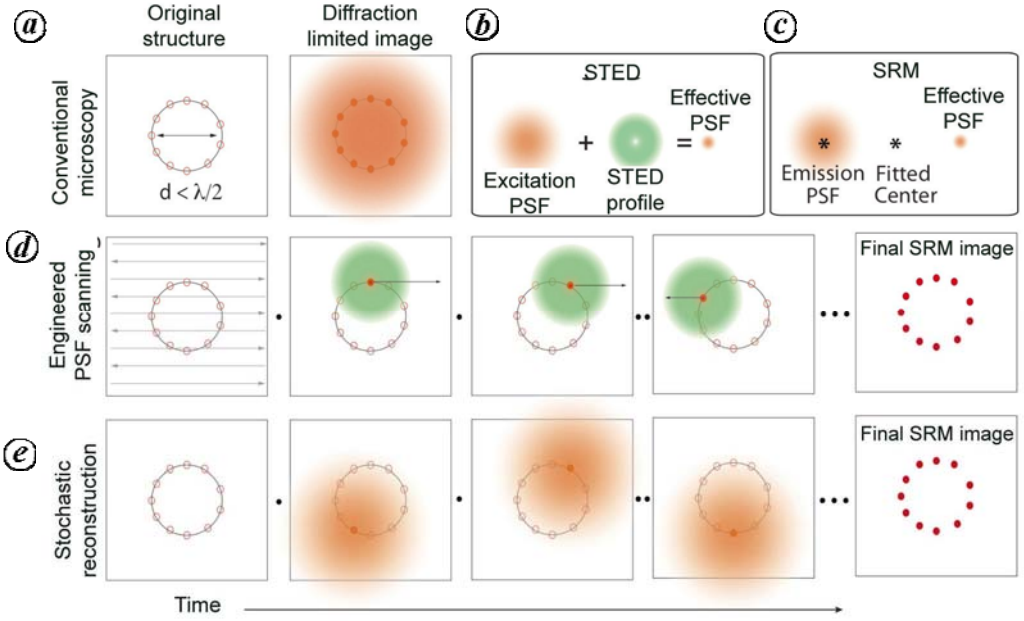

Figure 2. General principle for super-resolution microscopy. ***a***, Imaging a structure beyond the resolution limit *d* is challenging because, when all markers on the structure are emitting light, their individual PSFs overlap each other, hence blurring out the nanoscopic feature. ***b***, The key idea behind the major super-resolution techniques is to control the molecules emitting from a diffraction-limited spot by shuttling them between 'on' and 'off' states. Excitation PSF engineering and sequential readout techniques like RESOLFT rely on creating a narrow sub-region of excitation within the diffraction-limited spot. The rest of the surrounding region is switched to a non-emitting 'off' state with the help of overlapping switch-off laser with a donut beam profile featuring a central zero that overlaps the excitation maxima. ***c***, Stochastic reconstruction methods limit the number of emitters from a diffraction-limited region to close to one. Since the PSF of the emitter is known for the optical system, the fitting of this function can predict the accurate location of the molecule. ***d***, To create a super-resolution image in RESOLFT microscopy, the engineered PSF is scanned over the sample and the intensity of light collected from the sample is assigned to molecular density for that region. ***e***, Large sequence of images of the sample under conditions that allow only sparse number of the molecules to be turned 'on' is acquired and images processed to determine the positions of the 'on' molecules. The collated positions of the molecules from an image series are then used to reconstruct the final image.

ground state (dark state) before spontaneous emission can take place. To achieve sub-diffractive spatial selectivity in such a scheme, the STED laser is engineered to feature a spatial light intensity distribution, $I(r)$, with a central 'zero' intensity analogous to a donut shape (Figure 3 *a*). In the region away from r_0, as $I(r)$ values approach >> I_S, the saturation intensity for the simulated emission, larger fractions of molecules are set to the dark state. The full width half maximum (FWHM) of the narrowly confined region, *d*, and similarly, the new resolution of the system is now a function of STED beam intensity apart from the PSF of the optical system and is given by

$$d_{x,y} \approx \lambda / 2\eta \sin\alpha \sqrt{(1 + aI_{\max} / I_S)}, \quad (3)$$

where $I_{\max}$ is the peak intensity of the STED beam and *a* defines the properties of the intensity distribution[19]. Molecules that lie outside this central 'zero' region ($r > d/2$) are maintained in the dark state by stimulated emission and hence do not contribute to the signal even if they lie within $\lambda/2\eta$ distance from r_0. By scanning this STED beam configuration across the sample and collecting the signal that emanates only from the spatially constrained central region, one can now generate a super-resolution image.

Since the effective resolution *d* scales with the square root of $I_{\max}/I_S$ and I_S scales inversely with the lifetime of the 'on' and 'off' states, the switching mechanism and the choice of physical states lend different characteristics to the various members of this family of super-resolution techniques. For example, due to the short lifetimes (order of nanoseconds) for stimulated emission, the I_S values required are large (~ 50–200 MW/cm^2). In a related variant, ground state depletion (GSD) microscopy, the dark state is created by switching the molecules to triplet states or similar dark states (lifetimes ranging from millisecond to microsecond) and hence I_S values 3–6 orders smaller can be employed[22,25] (Figure 3 *b*). More recently, RESOLFT concept has been extended to switchable fluorescent proteins or organic dyes[26–28]. Most of these probes rely on photoinduced conformational change of the molecule to nonfluorescent 'dark' states that can be induced by low intensities (I_S ~ 1–80 kW/cm^2; Figure 3 *c*). The biggest challenges associated with RESOLFT with photoswitchable proteins for live samples were the slow kinetics of switching 'off' and the limited number of

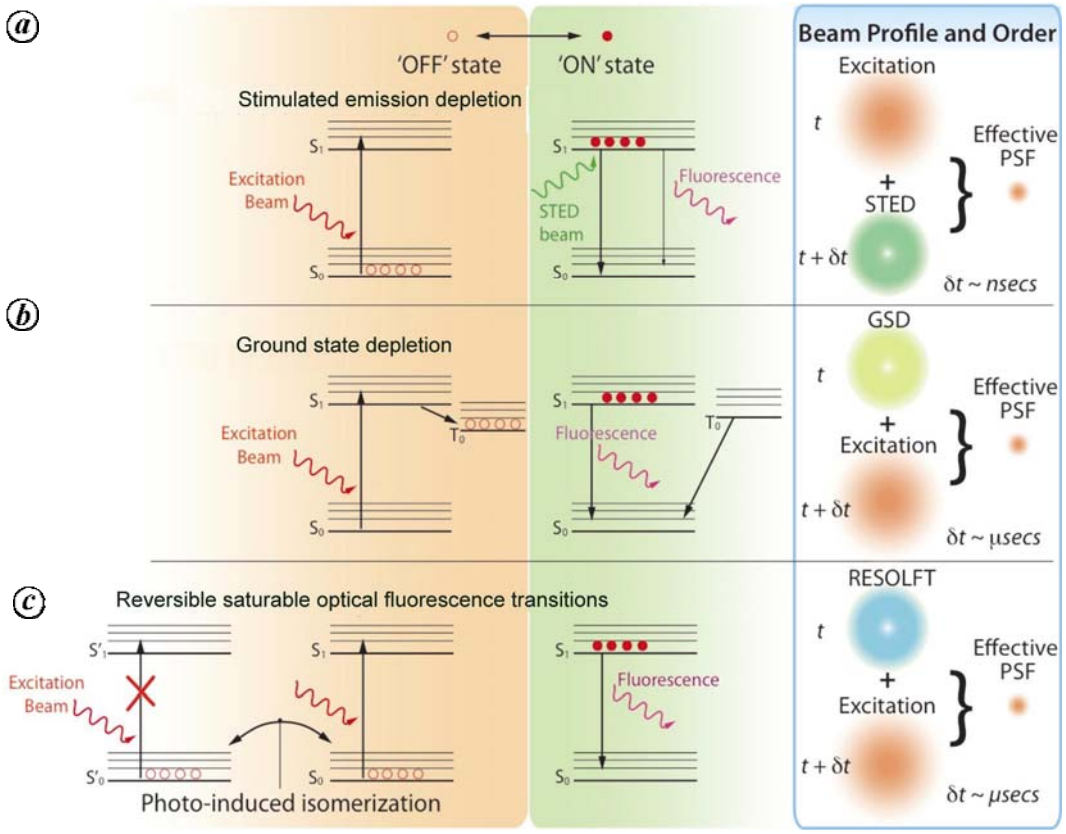

Figure 3. Various RESOLFT implementation schemes. ***a***, Stimulated emission depletion (STED) microscopy employs a red-shifted STED laser to pump the molecules from excited 'on' state to ground 'off' state before the molecule can emit a photon. The sample can be simultaneously scanned with excitation and STED laser and the resolution is determined by the peak power of the STED employed. ***b***, Ground state depletion (GSD) microscopy uses a single wavelength of laser, first at high intensity shaped as a donut to switch-off molecules by pushing them to triplet states and hence depleting the molecules in ground state and then using the excitation laser to collect light from the remaining molecules (in the central zero of the donut). ***c***, Reversible saturatable optical fluorescence transitions (RESOLFT) microscopy first generates a photoinduced isomerization of the molecules to long-lived dark states. The light is now collected from the remaining 'on' molecules in the central zero node by illuminating the region with the excitation beam.

'on–off' cycles making it slow and non-viable for long-term imaging respectively. These issues are being addressed by the development of a newer generation of reversibly switchable fluorescent proteins (RSFPs) that can speed up and extend continuous imaging by up to two orders of magnitude[29].

Stochastic localization and reconstruction microscopy (PALM, STORM, FPALM, PALMIRA)

Another approach to achieving higher resolution relies not on modifying the PSF of the system, but utilizing the prior knowledge of it to deconvolute the image. This technique works best under sparse label conditions where the number of molecules per diffraction-limited spot is close to one[2,21]. To achieve such imaging conditions and yet extend such imaging to any density of labels in the sample, several innovative schemes were employed by various groups independently[30–32]. The key idea, however, relies on a mechanism for stochastic switching of probes in the sample between 'dark' and 'emitting' states. Under conditions that allowed sparse population of single molecules to be in the 'emitting' state, acquired images of the sample could then be used to estimate position of the probe by fitting the image of the single molecules to an approximate PSF function, typically a two-dimensional Gaussian. Since the accuracy of locating the molecule position based on the PSF can be determined by the number of photons, N, as given by the relation

$$d_{x,y} = \lambda/2\eta \sin\alpha\sqrt{N}, \tag{4}$$

a 10–20X increase in the resolvability of point sources has been achieved for many fluorescent organic dyes and fluorescent proteins[1]. For generation of high-resolution images based on this principle, the process is repeated over many (occasionally several thousand) 'sparse' widefield images from a movie sequence and the final 'super-resolution' image reconstructed from the localized positions of the probes (Figure 2 *e*).

While the capability to locate molecules with high precision was conceptualized and demonstrated previously[18,33], the extension of the idea to microscopy was demonstrated with the control of the 'on–off' switching properties of the probes[30–32]. Originally, the activation to 'on' state was controlled by the action of low-intensity illumination (spectrally separate from excitation illumination), and then imaging performed on the activated molecules allowing for independent control over the timing, fraction and duration of activation. Generation of the 'dark' state by several mechanisms was employed. For example, teams led by Betzig and Hess used the photoactivation of fluorescent proteins from photoconversion to 'emitting/on' states[30,31]. On the other hand, the Zhuang group demonstrated that chemically induced 'dark' states in reducing conditions (by interaction of thiol groups with organic dyes) could be used to switch molecules to 'emitting' states in close proximity to another activator dye molecule (that was selectively illuminated by the activation laser)[32]. However, it was soon recognized that most fluorophores can undergo direct transition to 'dark' states under intense illumination or other chemical interactions and switch back to 'emitting' states by thermal or UV illumination, and hence diversifying and further simplifying the sample labelling schemes[34–43].

Axial super-resolution imaging

The need for three-dimensional microscopy is critical for biological imaging and yet imaging along the axial direction suffers from poor resolution. This has been addressed on two major fronts, namely super-resolution along the axial direction as well as the ability to achieve super-resolution imaging deep in the tissue by optical sectioning. While lateral super-resolution is achieved by PSF fitting, axial super-resolution has been achieved by projection of axial distances into lateral PSF functions. For example, the introduction of controlled astigmatism using a cylindrical lens in the emission optical path generates asymmetrical (elongated along one axis relative to the other) PSF depending upon the position of the molecule with respect to the axial focus (Figure 4 *a*). This elongated PSF of the blinking molecules can now be compared to calibrated single-molecule images to yield axial depth with 50 nm precision[44]. Similarly, the images can be split into two planes focused at different axial depths to allow estimation of the axial position based on the level of defocusing at the two planes[45] (Figure 4 *b*). Another approach relies on interference between the images of the molecules collected with two objectives such that the axial position of the molecules is encoded in the difference in the optical path-lengths[46]. This axial position is recovered by recombining the two beams from the objectives using a customized multiphase beamsplitter that generates three images with a mutual phase difference of ~120° (Figure 4 *c*). Furthermore, the single-molecule image can be split to generate a double-helix PSF using a spatial phase modulator, where the position and orientation of the two generated lobes can report on the 3D position of the molecules with a 10–20 nm accuracy[47,48] (Figure 4 *d*). Additional techniques that employ single-molecule reflections from tilted mirrors[49] or linear phase ramps in the objective pupil plane[50] can be selectively advantageous in terms of small depth of field imaging and ease of implementation respectively.

Deep tissue super-resolution imaging

Optical sectioning is inherently achieved in RESOLFT microscopy due to the underlying confocal scanning geometry. This allows easy extension to thick samples like tissue slices[51], nematodes[52] and living animal brain[53]. But aberrations arising from the system or sample can result in poor resolution or loss of signal. This can be countered with active feedback from adaptive optics-based PSF correction for thick living tissue to achieve aberration-free 3D imaging[54].

To effectively increase the vertical range of SRM microscopes, one needs to rely on selective illumination or activation in a 3D plane. Use of selective illumination using multiphoton excitation with temporal focusing[55] and light sheet-based illumination[56] has yielded selective activation and selective excitation deep in the biological sample respectively. To activate molecules selectively in a narrow *z*-plane of the sample, Vaziri and co-workers focused spectrally broadened short-pulses from a femtosecond laser onto the sample plane. Due to the nonlinear dependence of the two-photon absorption process, molecular excitation and activation probability is effectively limited to the narrow *z*-plane (order of a few microns) near the optical focus allowing selective activation of the photoactivatable fluorescent proteins. In a complementary approach, thin light sheets created either by Bessel beams[57] or cylindrical lenses[56] can be projected onto the sample using a perpendicular illumination objective in a plane orthogonal to the imaging objective and coplanar with its focal plane. By overlapping activation and excitation illuminations, one can selectively activate and excite single activatable molecules in this *z*-plane deep inside the tissue and apply stochastic reconstruction to achieve super-resolution imaging.

Multi-colour imaging

Interactions between various components of the cell are key to our understanding of cellular function. Traditionally, co-localization analysis of multi-colour fluorescence images has suffered because of limited resolution. For example, co-localization of arbitrarily shaped protein clusters is difficult to ascertain with ~200 nm resolution

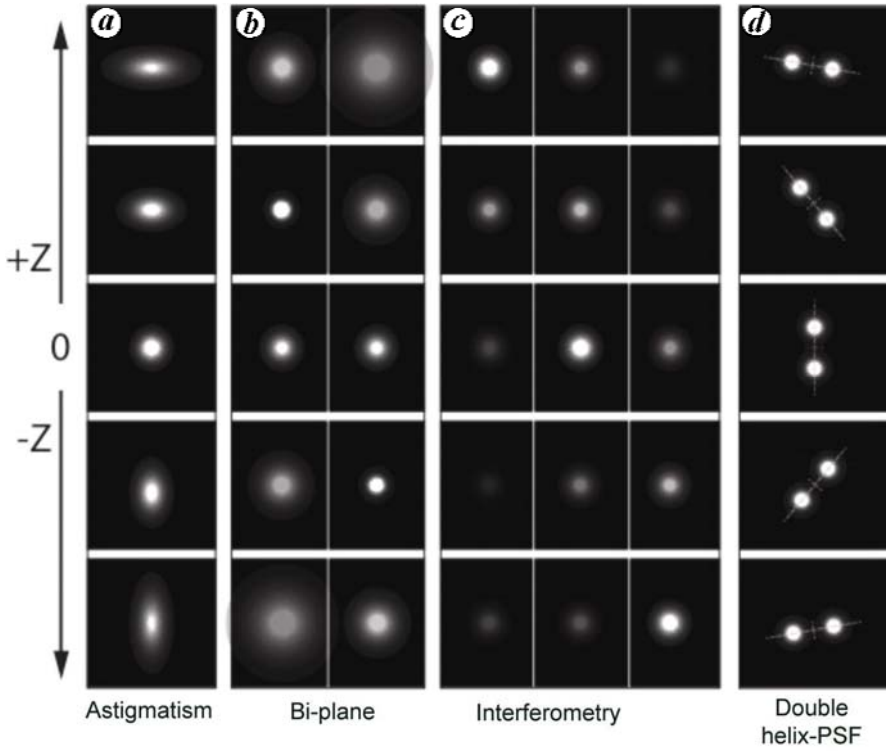

Figure 4. Super-axial resolution by stochastic reconstruction. The image series shows how the PSF of a single emitting molecule changes as a function of its axial position with respect to the focus ($Z = 0$) for various approaches to obtain axial resolution beyond the diffraction limit. ***a***, Astigmatism: A cylindrical lens in the emission path that modifies the focal distance along one axis creates an asymmetric PSF pattern. The ellipticity of the single-molecule image is a function of the *z*-position of the molecule and hence the *z*-position of the molecules can be determined by fitting the ellipticity to a precalibrated scale. ***b***, Bi-plane: Two images of single molecules are imaged simultaneously after splitting the emission path such that axial focus of the two is different. The level of defocusing in one channel versus the other defines the relative position of the molecule from the two focal planes. ***c***, Interferometry: Two simultaneous images of the sample molecules (usually using opposing objectives) are made to interfere with each other. The resulting images of the molecules change in intensity because of the optical path difference between the two emission paths. These images for different paths can be collected simultaneously for each molecule and the relative intensity for each segment will indicate the axial position of the molecule. ***d***, Double helix (DH)-PSF: Another unique approach relies on convolving the single molecule image with a DH-shaped PSF using Fourier optics and a reflective phase mask. The DH-PSF generates two spots on the CCD detector for each molecule. The lateral position of the emitter is determined by the mid-point between the two spots, whereas the orientation of the two spots is indicative of the axial position.

when overall features might overlap in conventional microscope images (Figure 5 *a*).

The biggest advantage of the 'on–off' schemes and availability of diverse probe choices has been in the extension of stochastic reconstruction microcopy for multi-colour imaging. It is now possible to either use a series of activator dyes in various combinations with reporter dyes providing selective activation for a set of molecules[58,59], or have spectrally distinct reporters and use thermal or photo-activation to image the cells in multi-colour[60–62]. As demonstrated in Figure 5 *b* and *c*, intricate organization of cellular components as in the case of endocytosis by clatharin-coated pits (CCPs) is revealed in live cells with unprecedented detail[63].

While more challenging in the case of STED microscopy, two-colour imaging was first demonstrated by the introduction of a spectrally distinct excitation and a corresponding STED laser[64]. In commercial STED systems, a single mode-locked Ti : sapphire laser is used to achieve stimulated emission for the pair of probes[65]. A more elegant approach for co-localization of two-colour imaging is achieved by employing fluorescent dyes with nearly identical absorption and emission spectra, but with different fluorescent lifetimes. In this case, the same excitation and STED beams illuminate both the dyes and the collected photons from the dyes are separated based on their lifetimes by a time-correlated single-photon counting (TCSPC) device allowing for simultaneous two-colour imaging[66]. Nevertheless, multi-colour STED imaging remains a high-investment endeavour and further development is needed in this area.

Super-resolution microscopy in biology

The potential impact of SRM is enormous and the technology has already started to contribute to biology disciplines. SRM has now percolated the wide spectrum of biological investigations that range from live animal

imaging[53] to single-cell transcriptomics[67]. The principal appeal of using fluorescence-based SRM has been its potential for live cell imaging. Though not fully applicable in all circumstances, especially when a high density of data points are required for reconstruction of the physical feature or cellular movements are comparable to acquisition time-frames, or long-term imaging of sample is required, SRM has been accomplished by several research groups in living mammalian cells[63,68–71]. Moreover, the added capability to specifically tag the molecule or structure of interest combined with multi-colour capabilities in these techniques is revolutionizing biological imaging[2,21,72].

Applications in cell biology

The best gains from SRM have been in cell biology that relies heavily upon imaging. With approximately tenfold better resolution, researchers have been imaging many of the cellular features that range from membrane architecture and dynamics[73,74] to chromosome conformation[75] that were close to the conventional resolution limit and needed such enhancement for better clarity. SRM has thus far been applied to resolve the cytoskeleton network in mammalian cells, cellular organelles like the endoplasic reticulum (ER), lysosome and mitochondria, as well as other cellular structures like nuclear pore complex and CCPs (reviewed in Huang *et al.*[21]).

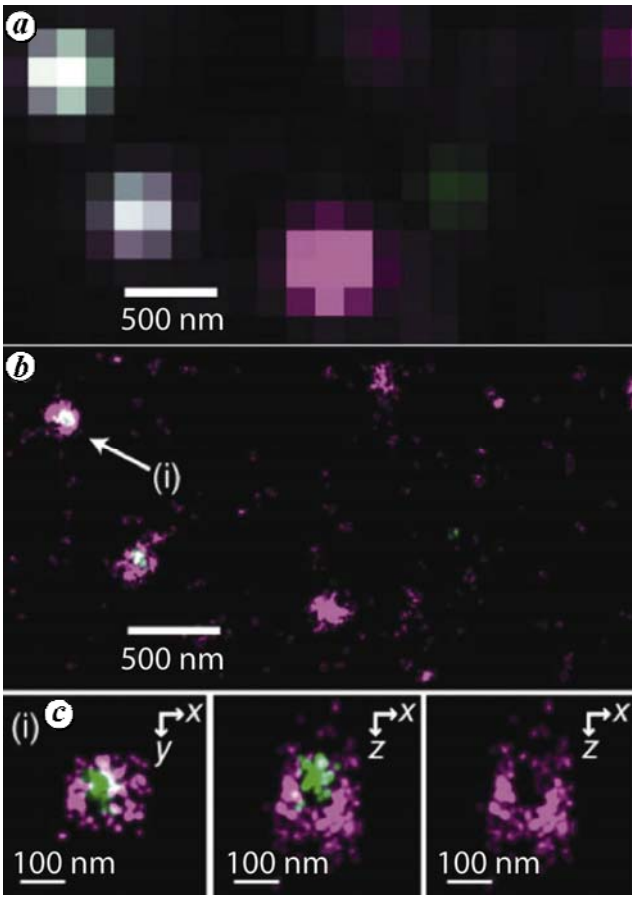

Figure 5. Multi-colour 3D stochastic reconstruction microscopy in live cells ***a***, Widefield two-colour image of clatharin-coated pits (CCPs) and transferrin in a live cell overlap spatially, such that no inference can be made regarding the actual nature of their interaction. ***b***, A 3D-SRM image (*x*–*y* projection, 30 s acquisition time) of the same region allows visualization of transferrin cargo in the interior of the CCP. ***c***, Zoomed images of a single CCP in *x*–*y* projection (left), *x*–*z* cross-section (middle), and *x*–*z* cross-section of clatharin channel only (right) show the cup shape of the pit near the plasma membrane. Adapted with permission from Macmillan Publishers Ltd, *Nature Methods*[63] © 2011.

A large fraction of the super-resolution techniques has investigated the cytoskeletal structure for proof-of-principle experiments due to known dimensions of microtubules. Interestingly, new spatial organizations of cytoskeletal components are being discovered. For example, actin, spectrin and adducin forms periodically arranged protein rings in axon shafts of cultured cells and brain tissue[76]. Another recent study used correlative single-molecule imaging and super-resolution imaging to probe how cargo transport occurred across microtubule intersections[77]. It showed that the cargo would pass or stall across the intersection in a separation distance-dependent manner with a transition in this behaviour at about 100 nm separation. Interestingly, an approaching cargo would generally maintain the same directionality after encountering the intersection, indicating that motor populations are stably associated with the cargo.

Super-resolution-based ultrastructure imaging of the multilaminar focal adhesion core that forms part of the cell anchorage to the surface[78] or the centrosome that serves as the platform for microtubule generation[79] also revealed how intricate arrangements of various components underlie their functional requirements. The dorsal and ventral sheets of actin filament network in cell protrusions were shown to have a different organization even when separated by 20–100 nm, suggesting that other molecules play a role in their ultrastructural organization[80].

Nanoscopic imaging of cell organelle organization has started to reveal how heterogeneous the distribution of cellular organelles and their constituents within the same organelle can be. For example, organization of mitochondria probed with STED microscopy[81], revealed how the components of the translocase complex of the mitochondrial outer membrane (TOM) are arranged in nano-sized clusters (30–40 nm). Their distribution is dependent on the membrane potential, cell growth conditions as well as the position of the cell within a colony. Similarly, the voltage-dependent anion channel (VDAC) proteins show heterogeneous clustered distribution of their various isoforms[82]. Remarkably, co-localization of the cytosolic protein hexokinase-I known to bind to the VDACs was demonstrated with the form of VDAC that remains bound on the surface of the mitochondria exclusively. As the capabilities of super-resolution techniques grow, more detailed information about various molecular complexes

in the living cell will improve the interpretation of images acquired at subpar resolution of conventional microscopes.

Applications neurobiology

Another related area that has received great impetus from SRM is neurobiology[72,83–86]. Optical SRM methods are now allowing researchers to probe the morphology and dynamics of neurons[87], dynamics of synaptic vesicles[88], and organization and localization of membrane fusion proteins[89–91]. For example, investigation of synaptic vesicles (30–50 nm in diameter) organization and dynamics has been the most illuminating. Essential protein components of these vesicles, such as the synaptotagmins and the SNARE proteins were discovered to be clustered in the plasma membrane while being in equilibrium with the free pool of mobile proteins[89,91,92]. SNARE proteins like syntaxin-1 and SNAP-25 clusters will colocalize with munc 18-1 suggesting possible mechanism for vesicle fusion[93].

Similarly, many aspects regarding the molecular architecture of synaptic junctions have been established. The proposed molecular organizer protein, Bruchpilot in *Drosophila* synapses was found localized in a donut shape around the active zones for vesicle release and promoting zone assembly and vesicle release[94]. Another study showed how presynaptic scaffolding proteins are differentially compartmentalized and spatially oriented with respect to the trans-synaptic axis[90]. Multi-colour labelling and high-throughput imaging of pre-synaptic active zone and post-synaptic density matrix proteins allowed determination of the position of the various proteins with respect to the synaptic cleft and showed a large inter-neuronal variability in the receptor composition and distribution.

The dynamic plasticity of dendritic spines with 60–80 nm resolution has been imaged in brain tissue slices[87,95] as well as living brain[53]. RESOLFT-based imaging of these spines can be carried out for several hours and chemical stimulants-based morphological changes could be followed[96]. Newer versions of reversibly switchable fluorescent proteins[29] should further increase the imaging speeds and total number of time-points in these studies paving the path for real-time imaging of dendritic plasticity at high resolution.

Applications in microbiology

Much of microbiology was in great need for super-resolution techniques for live cell imaging. Microbial ultrastructure and protein and nucleic acid spatio-temporal distributions have been addressed in several cases. Since excellent reviews exist[97–99], I will highlight only a few cases where novel insight was generated. In all the cases, we are increasingly finding out that small microbes are not merely bags packed with biomolecules, but have a high degree of ultrastructural organization.

Imaging of spatial distribution of the chemotaxis proteins in bacteria with SRM showed that these proteins do not form uniform or characteristic-sized clusters and the observed exponential distribution of the cluster sizes could be well explained by stochastic self-assembly without requiring direct cytoskeletal involvement or active transport[100]. On the other hand, several distinct structures like the FtsZ rings[101], MreB filaments[28,34] and ParA bundle[102] within the bacterial cell show how organization is critical to cell function.

Even for bacterial genome that was previously thought to exist as a loosely packed structure in the cell centre, new levels of the organization are being suggested based on new SRM studies. Wang *et al.*[103] demonstrated that nucleoid associated protein (NAP), H-NS actually forms distinct clusters in *Escherichia coli* in the nucleoid and their number, size and spatial distribution is a function of cell cycle and growth conditions. In combination with chromosome-conformation capture (3C) technique, they suggested that H-NS clustering might be inducing long-range chromatin interactions. Similar clusters of another NAP, namely HU have been found in *Caulobacter crescentus*, suggesting the universality of the genome organization in bacteria[104].

Another field of interest for application of SRM techniques would be the study of microbial ecosystems, where the large but closely packed cell populations make it difficult to discern molecular architecture. For example, by imaging matrix proteins in *Vibrio cholerae* biofilms, Berk *et al.*[105] demonstrated that cells would arrange in a hierarchical order of individual cells, cell clusters and a composite of clusters. More importantly, the different matrix proteins would play distinct roles like cell–cell adhesion and biofilm-to-surface adhesion. The cell clusters would be encased in a deformable and heterogeneous envelope of matrix proteins allowing for cell growth while maintaining integrity.

Applications in virology

While super-resolution virus imaging is still in its infancy, study of viral dynamic processes has the most to gain from real-time super-resolution techniques, since optical microscopy is now available at the appropriate length scales[30,106,107]. Most of the current work has been done for HIV studies, though the ideas are equally applicable to other viruses as long as fluorescent reagents that allow virus components to be labelled are available. With increasing improvements in resolution, speed and probes, we expect to see rapid growth in virus-imaging studies by SRM.

To study virion morphology and protein distribution, the virus proteins were tagged by small tetracysteine motifs that bind the fluorescein arsenical helix binder (FIAsH)[108] enabling localization-based SRM while maintaining virus

infectivity[109]. Mature conical cores that are 100 nm long could be distinguished from immature Gag shells and the virus integrase protein was shown to be mostly present encapsidated in the cytoplasm of the infected cells. In another study, maturation-induced clustering of the HIV envelope proteins was detected with STED microscopy[110]. Coupling of the virus envelope and Gag proteins allowed a correlated enhancement in virus infectivity during structural rearrangements of the inner structural proteins. Another super-resolution study with photoactivable fluorescent proteins allowed probing virus–host interactions with multi-colour SRM[111]. Vincent Piguet and colleagues found that the cellular restriction host-factor tetherin was mostly clustered around the HIV-1 assembly sites and this clustering was mediated by the transmembrane domain interactions, but was not associated with lipid raft domains unlike popular belief. Another study further looked at the nascent assembly of the two major components of the HIV-1 structure, namely the Gag and Env proteins[112]. It showed that Env glycoproteins recruitment occurred at the surroundings of Gag assembly sites and was dependent on Env cytoplasmic tail and other HIV proteins, suggesting unknown mechanisms for their co-assembly in the virion. These nascent SRM works would likely inspire more viral assembly, packaging, genome release and membrane fusion studies in the future.

Challenges

In spite of the strides in the attainable resolution and wide applicability demonstrated, there are several obstacles that lie ahead in SRM and further innovations will be necessary to overcome them. Many of the challenges like degree of labelling density, new probe development, sample preparation artifacts, limited speed and depth of field in dense and thick 3D samples, long-term continuous imaging, sample drift and vibrations and accurate molecular quantification as discussed previously[21,72,99], will need sustained efforts. Moreover, increased adaptability, portability and affordability of such systems in terms of inexpensive hardware for RESOLFT techniques and efficient software for single-molecule localization techniques will assist the growth in this area. One challenge that microscopy experts will have to guard against is the misinterpretation of SR data if one is not aware about the basic technical details. For example, in single-molecule localization-based microscopy repeated blinking of the probes results in clustered appearance in the reconstructed images. Careful analysis by a growing number of appropriate tools[113,114] should be carried out in SRM to avoid abuse of the technology.

The future

The focus of biology has long shifted from the study of morphology and phenotypic understanding of the organism to understanding of the underlying molecular mechanisms. This has been greatly aided by tools to target molecules specifically or purify them to homogeneity. In microscopy, development of optical probes and the discovery of genetically encodable fluorescent tags like GFP have allowed visualization of almost all aspects of the biochemical processes. As this focus transcends to '-omics' approaches, there is a greater demand on microscopy to probe multiple populations at the same time. This has been limiting in fluorescence microscopy, due to the lack of good spectrally separable probes and the broad nature of the excitation and emission spectra. Spurred by increased interest in a new generation of optical microscopy techniques and development of new probes, it is expected that multiple molecular populations (order of tens to hundreds) would be simultaneously probed and localized within single cells or organelles with nanometre precision.

These optical SR techniques are also technically challenging when it comes to molecular resolution. However, it is possible to obtain sub-nanometre localization between two separate optical probes[115] and hence it is only a matter of time when structural features of proteins and molecular complexes will be studied with SRM. Moreover, diffusional properties, co-localization, stoichiometry and orientation of molecules[116] would be additional useful readouts in the next installments of SRM.

A need to measure a functional property like charge, force or chemical state of a molecule rather than its physical location is essential to many problems. While this has more to do with the probe or assay development aspect of imaging, innovations in SRM are going to incite new approaches in this direction. Therefore, mapping the dynamics of an electrical potential propagation[117], quantitative estimates of the molecular forces[118], pH distribution[119] or fluid dynamics[120] within the cell will now be addressed at the nanometre level.

While most published SRM studies till now have demonstrated proof-of-principle concepts, rapid accessibility due to commercialization of these techniques is going to increase their impact in biology and undoubtedly generate novel insights. Since most of the techniques are based on fluorescence technology, all epi-fluorescence and/or confocal microscopes will probably be upgradeable to SRMs in the future. Biological imaging has taken a giant leap and only time will tell how far it takes us.

1. Fernandez-Suarez, M. and Ting, A. Y., Fluorescent probes for super-resolution imaging in living cells. *Nature Rev. Mol. Cell Biol.*, 2008, **9**, 929–943; doi: 10.1038/nrm2531.
2. Patterson, G., Davidson, M., Manley, S. and Lippincott-Schwartz, J., Superresolution imaging using single-molecule localization. *Annu. Rev. Phys. Chem.*, 2010, **61**, 345–367; doi: 10.1146/annurev.physchem.012809.103444.
3. Vaughan, J. C. and Zhuang, X., New fluorescent probes for super-resolution imaging. *Nature Biotechnol.*, 2011, **29**, 880–881; doi:10.1038/nbt.1997.

4. Vogelsang, J. *et al.*, Make them blink: probes for super-resolution microscopy. *ChemPhysChem*, 2010, **11**, 2475–2490; doi: 10.1002/cphc.201000189.
5. Hooke, R., *Micrographia* (eds Martyn, J. and Allestry, J.), 1st edn, 1665.
6. Dollond, J., Account of some experiments concerning the different refrangibility of light. *Philos. Trans. R. Soc.* (*London*), 1757, **50**, 733–743.
7. Lister, J. J., On some properties in achromatic object-glasses applicable to the improvement of the microscope. *Philos. Trans. R. Soc*., 1830, **120**, 187–200.
8. Abbe, E., Contributions to the theory of the microscope and microscopic observations (translated from German). *Arch. Mikrosk. Anat*., 1873, **9**, 413–468.
9. Pawley, J. B., *Handbook of Biological Confocal Microscopy*, Springer, New York, 2006, 3rd edn.
10. Hell, S. W., Far-field optical nanoscopy. *Science*, 2007, **316**, 1153–1158; doi: 10.1126/science.1137395.
11. Abbe, E., The relation of aperture and power in the microscope. *J. R.. Microscop. Soc*., 1883, **3**, 790–812.
12. Novotny, L. and Hecht, B., *Principles of Nano-Optics*, Cambridge University Press, 2006.
13. Gustafsson, M. G. L., Agard, D. A. and Sedat, J. W., (IM)-M-5: 3D widefield light microscopy with better than 100 nm axial resolution. *J. Microsc.-Oxford*, 1999, **195**, 10–16.
14. Hell, S. and Stelzer, E. H. K., Fundamental improvement of resolution with a 4pi-confocal fluorescence microscope using 2-photon excitation. *Opt. Commun*., 1992, **93**, 277–282; doi: 10.1016/0030-4018(92)90185-T.
15. Gustafsson, M. G., Surpassing the lateral resolution limit by a factor of two using structured illumination microscopy. *J. Microsc*., 2000, **198**, 82–87.
16. Planchon, T. A. *et al.*, Rapid three-dimensional isotropic imaging of living cells using Bessel beam plane illumination. *Nat. Methods*, 2011, **8**, U417–U468; doi: 10.1038/Nmeth.1586.
17. Gustafsson, M. G., Nonlinear structured-illumination microscopy: wide-field fluorescence imaging with theoretically unlimited resolution. *Proc. Natl. Acad. Sci., USA*, 2005, **102**, 13081–13086; doi: 10.1073/pnas.0406877102.
18. Yildiz, A. *et al.*, Myosin V walks hand-over-hand: single fluorophore imaging with 1.5-nm localization. *Science*, 2003, **300**, 2061–2065; doi: 10.1126/science.1084398.
19. Hell, S. W., Microscopy and its focal switch. *Nat. Methods*, 2009, **6**, 24–32; doi: 10.1038/nmeth.1291.
20. Hell, S. W. and Wichmann, J., Breaking the diffraction resolution limit by stimulated emission: stimulated–emission–depletion fluorescence microscopy. *Opt. Lett*., 1994, **19**, 780–782.
21. Huang, B., Bates, M. and Zhuang, X., Super-resolution fluorescence microscopy. *Annu. Rev. Biochem*., 2009, **78**, 993–1016; doi: 10.1146/annurev.biochem.77.061906.092014.
22. Hell, S. W. and Kroug, M., Ground-state-depletion fluorescence microscopy – a concept for breaking the diffraction resolution limit. *Appl. Phys. B – Lasers O*, 1995, **60**, 495–497; doi: 10.1007/Bf01081333.
23. Hell, S. W., Toward fluorescence nanoscopy. *Nature Biotechnol.*, 2003, **21**, 1347–1355; doi: 10.1038/nbt895.
24. Klar, T. A. and Hell, S. W., Subdiffraction resolution in far-field fluorescence microscopy. *Opt. Letts*., 1999, **24**, 954–956.
25. Bretschneider, S., Eggeling, C. and Hell, S. W., Breaking the diffraction barrier in fluorescence microscopy by optical shelving. *Phys. Rev. Letts*., 2007, **98**, 218103.
26. Hofmann, M., Eggeling, C., Jakobs, S. and Hell, S. W., Breaking the diffraction barrier in fluorescence microscopy at low light intensities by using reversibly photoswitchable proteins. *Proc. Natl. Acad. Sci. USA*, 2005, **102**, 17565–17569; doi: 10.1073/pnas.0506010102.
27. Bossi, M., Folling, J., Dyba, M., Westphal, V. and Hell, S. W., Breaking the diffraction resolution barrier in far-field microscopy by molecular optical bistability. *New J. Phys*., 2006, **8**, 275; doi: 10.1088/1367-2630/8/11/275.
28. Grotjohann, T. *et al.*, Diffraction-unlimited all-optical imaging and writing with a photochromic GFP. *Nature*, 2011, **478**, 204–208; doi: 10.1038/nature10497.
29. Grotjohann, T. *et al.*, rsEGFP2 enables fast RESOLFT nanoscopy of living cells. *eLife*, 2012, **1**, e00248; doi: 10.7554/eLife.00248.
30. Betzig, E. *et al.*, Imaging intracellular fluorescent proteins at nanometre resolution. *Science*, 2006, **313**, 1642–1645; doi: 10.1126/science.1127344.
31. Hess, S. T., Girirajan, T. P. and Mason, M. D., Ultra-high resolution imaging by fluorescence photoactivation localization microscopy. *Biophys. J*., 2006, **91**, 4258–4272; doi: 10.1529/biophysj.106.091116.
32. Rust, M. J., Bates, M. and Zhuang, X., Sub-diffraction-limit imaging by stochastic optical reconstruction microscopy (STORM). *Nat. Methods*, 2006, **3**, 793–795; doi: 10.1038/nmeth929.
33. Thompson, R. E., Larson, D. R. and Webb, W. W., Precise nanometre localization analysis for individual fluorescent probes. *Biophys. J.*, 2002, **82**, 2775–2783; doi: 10.1016/S0006-3495(02)75618-X.
34. Biteen, J. S. *et al.* Super-resolution imaging in live *Caulobacter crescentus* cells using photoswitchable EYFP. *Nat. Methods*, 2008, **5**, 947–949; doi: 10.1038/nmeth.1258.
35. Heilemann, M. *et al.*, Subdiffraction-resolution fluorescence imaging with conventional fluorescent probes. *Angew. Chem*., 2008, **47**, 6172–6176; doi: 10.1002/anie.200802376.
36. Baddeley, D., Jayasinghe, I. D., Cremer, C., Cannell, M. B. and Soeller, C., Light-induced dark states of organic fluochromes enable 30 nm resolution imaging in standard media. *Biophys. J*., 2009, **96**, L22–L24; doi: 10.1016/j.bpj.2008.11.002.
37. Lee, H. L. D. *et al.*, Superresolution imaging of targeted proteins in fixed and living cells using photoactivatable organic fluorophores. *J. Am. Chem. Soc*., 2010, **132**, 15099–15101; doi: 10.1021/Ja1044192.
38. Lemmer, P. *et al.*, Using conventional fluorescent markers for far-field fluorescence localization nanoscopy allows resolution in the 10-nm range. *J. Microsc.-Oxford*, 2009, **235**, 163–171.
39. Dempsey, G. T., Vaughan, J. C., Chen, K. H., Bates, M. and Zhuang, X., Evaluation of fluorophores for optimal performance in localization-based super-resolution imaging. *Nat. Methods*, 2011, **8**, 1027–1036; doi: 10.1038/nmeth.1768.
40. Shim, S. H. *et al.*, Super-resolution fluorescence imaging of organelles in live cells with photoswitchable membrane probes. *Proc. Natl. Acad. Sci., USA*, 2012, **109**, 13978–13983; doi: 10.1073/pnas.1201882109.
41. Folling, J. *et al.*, Fluorescence nanoscopy by ground-state depletion and single-molecule return. *Nat. Methods*, 2008, **5**, 943–945, doi: 10.1038/Nmeth.1257.
42. Burnette, D. T., Sengupta, P., Dai, Y. H., Lippincott-Schwartz, J. and Kachar, B., Bleaching/blinking assisted localization microscopy for superresolution imaging using standard fluorescent molecules. *Proc. Natl. Acad. Sci., USA*, 2011, **108**, 21081–21086; doi: 10.1073/Pnas.1117430109.
43. Sharonov, A. and Hochstrasser, R. M., Wide-field subdiffraction imaging by accumulated binding of diffusing probes. *Proc. Natl. Acad. Sci. USA*, 2006, **103**, 18911–18916; doi: 10.1073/Pnas.0609643104.
44. Huang, B., Wang, W., Bates, M. and Zhuang, X., Three-dimensional super-resolution imaging by stochastic optical reconstruction microscopy. *Science*, 2008, **319**, 810–813; doi: 10.1126/science.1153529.
45. Juette, M. F. *et al.*, Three-dimensional sub-100 nm resolution fluorescence microscopy of thick samples. *Nat. Methods*, 2008, **5**, 527–529; doi: 10.1038/nmeth.1211.

46. Shtengel, G. *et al.*, Interferometric fluorescent super-resolution microscopy resolves 3D cellular ultrastructure. *Proc. Natl. Acad. Sci. USA*, 2009, **106**, 3125–3130; doi: 10.1073/pnas.0813131106.
47. Pavani, S. R. *et al.*, Three-dimensional, single-molecule fluorescence imaging beyond the diffraction limit by using a double-helix point spread function. *Proc. Natl. Acad. Sci. USA*, 2009, **106**, 2995–2999; doi: 10.1073/pnas.0900245106.
48. Grover, G., DeLuca, K., Quirin, S., DeLuca, J. and Piestun, R. Super-resolution photon-efficient imaging by nanometric double-helix point spread function localization of emitters (SPINDLE). *Opt. Express*, 2012, **20**, 26681–26695; doi: 10.1364/OE.20.026681.
49. Tang, J., Akerboom, J., Vaziri, A., Looger, L. L. and Shank, C. V., Near-isotropic 3D optical nanoscopy with photon-limited chromophores. *Proc. Natl. Acad. Sci. USA*, 2010, **107**, 10068–10073; doi: 10.1073/pnas.1004899107.
50. Baddeley, D., Cannell, M. and Soeller, C., Three-dimensional sub-100 nm super-resolution imaging of biological samples using a phase ramp in the objective pupil. *Nano Res*., 2011, **4**, 589–598; doi: 10.1007/S12274-011-0115-Z.
51. Ding, J. B., Takasaki, K. T. and Sabatini, B. L., Supraresolution imaging in brain slices using stimulated-emission depletion two-photon laser scanning microscopy. *Neuron*, 2009, **63**, 429–437; doi: 10.1016/j.neuron.2009.07.011.
52. Rankin, B. R. *et al.*, Nanoscopy in a living multicellular organism expressing GFP. *Biophys. J*., 2011, **100**, L63–L65; doi: 10.1016/j.bpj.2011.05.020.
53. Berning, S., Willig, K. I., Steffens, H., Dibaj, P. and Hell, S. W., Nanoscopy in a living mouse brain. *Science*, 2012, **335**, 551; doi: 10.1126/science.1215369.
54. Gould, T. J., Burke, D., Bewersdorf, J. and Booth, M. J., Adaptive optics enables 3D STED microscopy in aberrating specimens. *Opt. Exp*., 2012, **20**, 20998–21009.
55. Vaziri, A., Tang, J., Shroff, H. and Shank, C. V., Multilayer three-dimensional super resolution imaging of thick biological samples. *Proc. Natl. Acad. Sci. USA*, 2008, **105**, 20221–20226; doi: 10.1073/pnas.0810636105.
56. Zanacchi, F. C. *et al.*, Live-cell 3D super-resolution imaging in thick biological samples. *Nat. Methods*, 2011, **8**, 1047; doi: 10.1038/Nmeth.1744.
57. Gao, L. *et al.*, Noninvasive Imaging beyond the diffraction limit of 3D dynamics in thickly fluorescent specimens. *Cell*, 2012, **151**, 1370–1385; doi: 10.1016/J.Cell.2012.10.008.
58. Bates, M., Huang, B., Dempsey, G. T. and Zhuang, X., Multicolour super-resolution imaging with photo-switchable fluorescent probes. *Science*, 2007, **317**, 1749–1753; doi: 10.1126/science.1146598.
59. Bates, M., Dempsey, G. T., Chen, K. H. and Zhuang, X., Multicolour super-resolution fluorescence imaging via multi-parameter fluorophore detection. *ChemPhysChem*, 2012, **13**, 99–107; doi: 10.1002/cphc.201100735.
60. Shroff, H. *et al.*, Dual-colour superresolution imaging of genetically expressed probes within individual adhesion complexes. *Proc. Natl. Acad. Sci. USA*, 2007, **104**, 20308–20313; doi: 10.1073/pnas.0710517105.
61. Baddeley, D. *et al*., 4D Super-resolution microscopy with conventional fluorophores and single wavelength excitation in optically thick cells and tissues. *PLoS One*, 2011, **6**, e20645; doi: 10.1371/journal.pone.0020645.
62. Testa, I. *et al.*, Multicolour fluorescence nanoscopy in fixed and living cells by exciting conventional fluorophores with a single wavelength. *Biophys. J*., 2010, **99**, 2686–2694; doi: 10.1016/j.bpj.2010.08.012.
63. Jones, S. A., Shim, S. H., He, J. and Zhuang, X., Fast, three-dimensional super-resolution imaging of live cells. *Nature Methods*, 2011, **8**, 499–508; doi: 10.1038/nmeth.1605.
64. Donnert, G. *et al.*, Two-colour far-field fluorescence nanoscopy. *Biophys. J*., 2007, **92**, L67–L69; doi: 10.1529/biophysj.107.104497.
65. Pellett, P. A. *et al.*, Two-colour STED microscopy in living cells. *Biomed. Opt. Express*, 2011, **2**, 2364–2371.
66. Buckers, J., Wildanger, D., Vicidomini, G., Kastrup, L. and Hell, S. W., Simultaneous multi-lifetime multi-colour STED imaging for colocalization analyses. *Opt. Express*, 2011, **19**, 3130–3143; doi: 10.1364/Oe.19.003130.
67. Lubeck, E. and Cai, L., Single-cell systems biology by super-resolution imaging and combinatorial labeling. *Nat. Methods*, 2012, **9**, 743–748; doi: 10.1038/nmeth.2069.
68. Benke, A. and Manley, S., Live-cell dSTORM of cellular DNA based on direct DNA labeling. *ChemBioChem*, 2012, **13**, 298–301; doi: 10.1002/cbic.201100679.
69. Klein, T. *et al.*, Live-cell dSTORM with SNAP-tag fusion proteins. *Nat. Methods*, 2011, **8**, 7–9; doi: 10.1038/nmeth0111-7b.
70. Wombacher, R. *et al.*, Live-cell super-resolution imaging with trimethoprim conjugates. *Nat. Methods*, 2010, **7**, 717–719; doi: 10.1038/nmeth.1489.
71. Shroff, H., Galbraith, C. G., Galbraith, J. A. and Betzig, E., Live-cell photoactivated localization microscopy of nanoscale adhesion dynamics. *Nat. Methods*, 2008, **5**, 417–423; doi: 10.1038/nmeth.1202.
72. Ji, N., Shroff, H., Zhong, H. and Betzig, E., Advances in the speed and resolution of light microscopy. *Curr. Opin. Neurobiol*., 2008, **18**, 605–616; doi: 10.1016/j.conb.2009.03.009.
73. Manley, S. *et al.*, High-density mapping of single-molecule trajectories with photoactivated localization microscopy. *Nat. Methods*, 2008, **5**, 155–157; doi: 10.1038/nmeth.1176.
74. Eggeling, C. *et al.*, Direct observation of the nanoscale dynamics of membrane lipids in a living cell. *Nature*, 2009, **457**, 1159–1162; doi: 10.1038/nature07596.
75. Flors, C. and Earnshaw, W. C., Super-resolution fluorescence microscopy as a tool to study the nanoscale organization of chromosomes. *Curr. Opin. Chem. Biol*., 2011, **15**, 838–844; doi: 10.1016/j.cbpa.2011.10.004.
76. Xu, K., Zhong, G. and Zhuang, X., Actin, spectrin, and associated proteins form a periodic cytoskeletal structure in axons. *Science*, 2013, **339**, 452–456; doi: 10.1126/science.1232251.
77. Balint, S., Verdeny Vilanova, I., Sandoval Alvarez, A. and Lakadamyali, M., Correlative live-cell and superresolution microscopy reveals cargo transport dynamics at microtubule intersections. *Proc. Natl. Acad. Sci. USA*, 2013, **110**, 3375–3380, doi: 10.1073/pnas.1219206110.
78. Kanchanawong, P. *et al*., Nanoscale architecture of integrin-based cell adhesions. *Nature*, 2010, **468**, 580–584, doi: 10.1038/nature09621.
79. Mennella, V. *et al.*, Subdiffraction-resolution fluorescence microscopy reveals a domain of the centrosome critical for pericentriolar material organization. *Nature Cell Biol*., 2012, **14**, 1159–1168; doi: 10.1038/ncb2597.
80. Xu, K., Babcock, H. P. and Zhuang, X., Dual-objective STORM reveals three-dimensional filament organization in the actin cytoskeleton. *Nat. Methods*, 2012, **9**, 185–188; doi: 10.1038/nmeth.1841.
81. Wurm, C. A. *et al.* Nanoscale distribution of mitochondrial import receptor Tom20 is adjusted to cellular conditions and exhibits an inner-cellular gradient. *Proc. Natl. Acad. Sci. USA*, 2011, **108**, 13546–13551; doi: 10.1073/pnas.1107553108.
82. Neumann, D., Buckers, J., Kastrup, L., Hell, S. W. and Jakobs, S., Two-colour STED microscopy reveals different degrees of colocalization between hexokinase-I and the three human VDAC isoforms. *PMC Biophys*., 2010, **3**, 4; doi: 10.1186/1757-5036-3-4.
83. Tonnesen, J. and Nagerl, U. V., Superresolution imaging for neuroscience. *Exp. Neurol*., 2013, **242**, 33–40; doi: 10.1016/j.expneurol.2012.10.004.
84. Sigrist, S. J. and Sabatini, B. L., Optical super-resolution microscopy in neurobiology. *Curr. Opin. Neurobiol*., 2012, **22**, 86–93; doi: 10.1016/j.conb.2011.10.014.

85. Saka, S. and Rizzoli, S. O., Super-resolution imaging prompts re-thinking of cell biology mechanisms: selected cases using stimulated emission depletion microscopy. *BioEssays*, 2012, **34**, 386–395; doi: 10.1002/bies.201100080.
86. Dani, A. and Huang, B., New resolving power for light microscopy: applications to neurobiology. *Curr. Opin. Neurobiol*., 2010, **20**, 648–652; doi: 10.1016/j.conb.2010.07.006.
87. Nagerl, U. V., Willig, K. I., Hein, B., Hell, S. W. and Bonhoeffer, T., Live-cell imaging of dendritic spines by STED microscopy. *Proc. Natl. Acad. Sci. USA*, 2008, **105**, 18982–18987; doi: 10.1073/pnas.0810028105.
88. Westphal, V. *et al*., Video-rate far-field optical nanoscopy dissects synaptic vesicle movement. *Science*, 2008, **320**, 246–249; doi: 10.1126/science.1154228.
89. Sieber, J. J. *et al*., Anatomy and dynamics of a supramolecular membrane protein cluster. *Science*, 2007, **317**, 1072–1076; doi: 10.1126/science.1141727.
90. Dani, A., Huang, B., Bergan, J., Dulac, C. and Zhuang, X., Superesolution imaging of chemical synapses in the brain. *Neuron*, 2010, **68**, 843–856; doi: 10.1016/j.neuron.2010.11.021.
91. Willig, K. I., Rizzoli, S. O., Westphal, V., Jahn, R. and Hell, S. W., STED microscopy reveals that synaptotagmin remains clustered after synaptic vesicle exocytosis. *Nature*, 2006, **440**, 935–939; doi: 10.1038/nature04592.
92. Sieber, J. J., Willig, K. I., Heintzmann, R., Hell, S. W. and Lang, T., The SNARE motif is essential for the formation of syntaxin clusters in the plasma membrane. *Biophys. J*., 2006, **90**, 2843–2851; doi: 10.1529/biophysj.105.079574.
93. Pertsinidis, A. *et al.*, Ultrahigh-resolution imaging reveals formation of neuronal SNARE/Munc 18 complexes *in situ*. *Proc. Natl. Acad. Sci. USA*, 2013, **110**, E2812–E2820.
94. Kittel, R. J. *et al*., Bruchpilot promotes active zone assembly, Ca^{2+} channel clustering, and vesicle release. *Science*, 2006, **312**, 1051–1054; doi: 10.1126/science.1126308.
95. Urban, N. T., Willig, K. I., Hell, S. W. and Nagerl, U. V., STED nanoscopy of actin dynamics in synapses deep inside living brain slices. *Biophys. J*., 2011, **101**, 1277–1284; doi: 10.1016/j.bpj.2011.07.027.
96. Testa, I. *et al.*, Nanoscopy of living brain slices with low light levels. *Neuron*, 2012, **75**, 992–1000; doi: 10.1016/j.neuron.2012.07.028.
97. Biteen, J. S. and Moerner, W. E., Single-molecule and superresolution imaging in live bacteria cells. *Cold Spring Harbor Perspectives in Biology*, 2010, **2**, a000448; doi: 10.1101/cshperspect.a000448.
98. Cattoni, D. I., Fiche, J. B. and Nollmann, M., Single-molecule super-resolution imaging in bacteria. *Curr. Opin. Microbiol*., 2012, **15**, 758–763; doi: 10.1016/j.mib.2012.10.007.
99. Coltharp, C. and Xiao, J., Superresolution microscopy for microbiology. *Cell. Microbiol*., 2012, **14**, 1808–1818; doi: 10.1111/cmi.12024.
100. Greenfield, D. *et al*., Self-organization of the *Escherichia coli* chemotaxis network imaged with super-resolution light microscopy. *PLOS Biol*., 2009, **7**, e1000137; doi: 10.1371/journal.pbio.1000137.
101. Fu, G. *et al.*, *In vivo* structure of the *E. coli* FtsZ-ring revealed by photoactivated localization microscopy (PALM). *PLoS One*, 2010, **5**, e12682; doi: 10.1371/journal.pone.0012680.
102. Ptacin, J. L. *et al*., A spindle-like apparatus guides bacterial chromosome segregation. *Nature Cell Biol*., 2010, **12**, 791–798; doi: 10.1038/ncb2083.
103. Wang, W., Li, G. W., Chen, C., Xie, X. S. and Zhuang, X., Chromosome organization by a nucleoid-associated protein in live bacteria. *Science*, 2011, **333**, 1445–1449; doi: 10.1126/science.1204697.
104. Lee, S. F., Thompson, M. A., Schwartz, M. A., Shapiro, L. and Moerner, W. E., Super-resolution imaging of the nucleoid-associated protein HU in *Caulobacter crescentus*. *Biophys. J*., 2011, **100**, L31–L33; doi: 10.1016/j.bpj.2011.02.022.
105. Berk, V. *et al.*, Molecular architecture and assembly principles of *Vibrio cholerae* biofilms. *Science*, 2012, **337**, 236–239l; doi: 10.1126/science.1222981.
106. Eckhardt, M. *et al.*, A SNAP-tagged derivative of HIV-1-A versatile tool to study virus-cell interactions. *PLoS One*, 2011, **6**, e22007; doi: 10.1371/journal.pone.0022007.
107. Willig, K. I. *et al.*, Nanoscale resolution in GFP-based microscopy. *Nat. Methods*, 2006, **3**, 721–723; doi: 10.1038/Nmeth922.
108. Griffin, B. A., Adams, S. R. and Tsien, R. Y., Specific covalent labeling of recombinant protein molecules inside live cells. *Science*, 1998, **281**, 269–272.
109. Lelek, M. *et al*., Superresolution imaging of HIV in infected cells with FlAsH-PALM. *Proc. Natl. Acad. Sci. USA*, 2012, **109**, 8564–8569; doi: 10.1073/pnas.1013267109.
110. Chojnacki, J. *et al.*, Maturation-dependent HIV-1 surface protein redistribution revealed by fluorescence nanoscopy. *Science*, 2012, **338**, 524–528; doi: 10.1126/science.1226359.
111. Lehmann, M. *et al*., Quantitative multicolour super-resolution microscopy reveals tetherin HIV-1 interaction. *PLoS Pathog*., 2011, **7**, E1002456; doi: 10.1371/Journal.Ppat.1002456.
112. Muranyi, W., Malkusch, S., Muller, B., Heilemann, M. and Krausslich, H. G., Super-resolution microscopy reveals specific recruitment of HIV-1 envelope proteins to viral assembly sites dependent on the envelope C-terminal tail. *PLoS Pathog*., 2013, **9**, e1003198; doi: 10.1371/journal.ppat.1003198.
113. Sengupta, P. and Lippincott-Schwartz, J., Quantitative analysis of photoactivated localization microscopy (PALM) datasets using pair-correlation analysis. *BioEssays*, 2012, **34**, 396–405; doi: 10.1002/bies.201200022.
114. Coltharp, C., Kessler, R. P. and Xiao, J., Accurate construction of photoactivated localization microscopy (PALM) images for quantitative measurements. *PLoS One*, 2012, **7**, e51725; doi: 10.1371/journal.pone.0051725.
115. Pertsinidis, A., Zhang, Y. X. and Chu, S., Subnanometre single-molecule localization, registration and distance measurements. *Nature*, 2010, **466**, 647–651; doi: 10.1038/nature09163.
116. Gould, T. J. *et al*., Nanoscale imaging of molecular positions and anisotropies. *Nat. Methods*, 2008, **5**, 1027–1030; doi: 10.1038/nmeth.1271.
117. Kralj, J. M., Douglass, A. D., Hochbaum, D. R., Maclaurin, D. and Cohen, A. E., Optical recording of action potentials in mammalian neurons using a microbial rhodopsin. *Nat. Methods*, 2012, **9**, 90–95; doi: 10.1038/nmeth.1782.
118. Grashoff, C. *et al.*, Measuring mechanical tension across vinculin reveals regulation of focal adhesion dynamics. *Nature*, 2010, **466**, 263–266; doi: 10.1038/nature09198.
119. Modi, S. *et al.*, A DNA nanomachine that maps spatial and temporal pH changes inside living cells. *Nature Nanotechnol*., 2009, **4**, 325–330; doi: 10.1038/nnano.2009.83.
120. Keren, K., Yam, P. T., Kinkhabwala, A., Mogilner, A. and Theriot, J. A., Intracellular fluid flow in rapidly moving cells. *Nature Cell Biol*., 2009, **11**, 1219–1224; doi: 10.1038/Ncb1965.

ACKNOWLEDGEMENTS. This work is supported by the Indian Institute of Science, Bangalore; Department of Science and Technology, New Delhi and the Innovative Young Biotechnologist award from the Department of Biotechnology, New Delhi.